Chem Biol Drug Des 2016; **87:** 569–574

Research Article

Design, Synthesis, and Biological Evaluation of 1-Benzyl-1*H*-pyrazole Derivatives as Receptor Interacting Protein 1 Kinase Inhibitors

Chan Zou[1,2,†], Yu Xiong[1,2,†], Lu-Yi Huang[1,2,†], Chun-Li Song[3], Xiao-Ai Wu[1,2], Lin-Li Li[3,*] and Sheng-Yong Yang[1,2,*]

[1]*State Key Laboratory of Biotherapy and Cancer Center, West China Hospital, Sichuan University, Chengdu, Sichuan 610041, China*
[2]*Collaborative Innovation Center of Biotherapy, Chengdu, Sichuan 610041, China*
[3]*West China School of Pharmacy, Sichuan University, Chengdu, Sichuan 610041, China*
**Corresponding authors: Lin-Li Li, ysylilinli@sina.com*; Sheng-Yong Yang, *yangsy@scu.edu.cn*
[†]*These authors contributed equally.*

Receptor interacting protein 1 (RIP1) kinase plays an important role in necroptosis, and inhibitors of the RIP1 kinase are thought to have a potential therapeutic value in the treatment of diseases related to necrosis. Herein, we report the structural optimization of a RIP1 kinase inhibitor, 1-(2,4-dichlorobenzyl)-3-nitro-1*H*-pyrazole (1a). A number of 1-benzyl-1H-pyrazole derivatives were synthesized and structure-activity relationship (SAR) analysis led to the discovery of a potent compound, 4b, which showed a K_d value of 0.078 μM against the RIP1 kinase and an EC_{50} value of 0.160 μM in a cell necroptosis inhibitory assay. Compound 4b also displayed considerable ability to protect the pancreas in an L-arginine-induced pancreatitis mouse model.

Key words: 1-benzyl-1*H*-pyrazoles, kinase, necroptosis, pancreatitis, receptor interacting protein 1

Received 14 June 2015, revised 4 November 2015 and accepted for publication 5 November 2015

Necrosis, an alternative form of programmed cell death, plays a prominent role in many pathological conditions, including ischemic brain injury (1), neurodegenerative diseases (2), heart ischemia/reperfusion injury (3), and viral infection (4,5). It has conventionally been viewed as an accidental and unwanted cell death, carried out in a non-regulated manner. However, recent studies have shown that necrosis can also be highly regulated in certain condition, hence termed necroptosis (6). The signaling pathway responsible for carrying out necroptosis has just been understood (7,8), and receptor interacting protein 1 (RIP1) kinase is thought to be one of the key regulators of necroptosis (9,10). RIP1 is a serine–threonine protein kinase and has been demonstrated to directly regulate RIP3-MLKL-dependent necroptosis (11); the RIP3-MLKL cascade is a driving signaling pathway leading to necroptosis recently discovered, which is triggered by death receptor such as tumor necrosis factor receptor (TNFR). Discovery of RIP1 kinase inhibitors could help in elucidating the regulation mechanism of necroptosis and might provide potential therapeutic agents for diseases related to necrosis.

Up to now, a number of RIP1 kinase inhibitors have been reported. Representative ones including Nec1 (12), Nec-3a (13), Nec-4 (14), Nec-5 (15), Nec-21 (16), and Cpd27 (17) are shown in Figure 1, and Nec1 is often used as a molecular tool in necroptosis-related studies (10). Even so, most of these compounds just showed moderate activity against the RIP1 kinase. Therefore, discovering more potent RIP1 kinase inhibitors, particularly those containing new chemical scaffolds, is still necessary at present.

We recently identified a new necroptosis inhibitor, namely 1-(2,4-dichlorobenzyl)- 3-nitro-1*H*-pyrazole (**1a**, Figure 2); the chemical scaffold contained in this compound, 1-Benzyl-1H-pyrazole, is a novel one, which means that 1-Benzyl-1H-pyrazole derivatives have never been reported as RIP1 kinase inhibitors. Compound **1a** was obtained through screening our in-house database by a cell necroptosis inhibitory assay, in which human colon cell line HT29 was treated with TNF-α, Smac mimetic, and Z-VAD-FMK (TSZ). Here, TNF-α and Smac mimetic can cause cells to undergo apoptosis by triggering the formation of a caspase-8 activating complex containing RIP1, and Z-VAD-FMK is a pan-caspase inhibitor and can switch apoptosis to necroptosis in RIP3-expressing cells upon caspase-8 inhibition (18). In this assay, Nec1 was used as a positive control, which displayed an EC_{50} (concentration for 50% of maximal effect) value of 0.860 μM. Compound **1a** exhibited an EC_{50} value of 1.048 μM. A further kinase inhibition assay showed that compound **1a** was a RIP1 kinase inhibitor with a K_d value of 0.130 μM and exhibited no inhibitory activity against RIP3. The purpose here is to further optimize its potency and carry out a structure-activity relationship (SAR) analysis.

© 2015 John Wiley & Sons A/S. doi: 10.1111/cbdd.12689

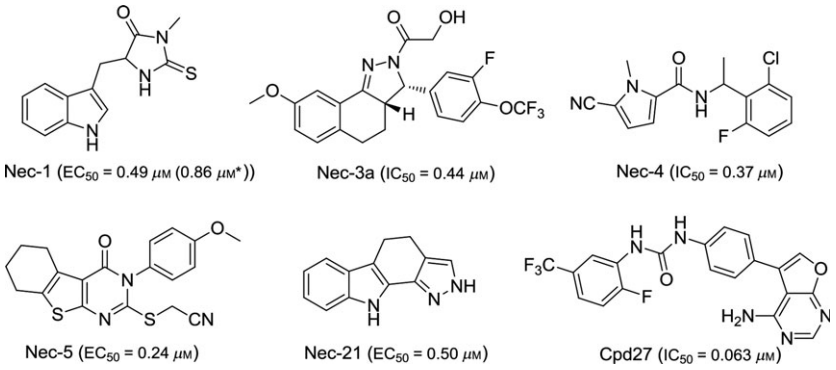

Figure 1: Structures of representative RIP1 kinase inhibitors together with their bioactivities (*EC_{50} obtained in this study).

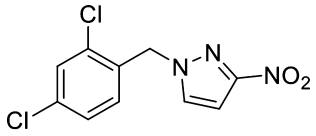

1a

Figure 2: The structure of hit compound **1a**.

Methods and Materials

General procedure for the synthesis of compounds 3a–3c (exemplified by 3a)

A solution of 3-nitro-1*H*-pyrazole (2.0 g, 17.7 mmol) and N-chloro-succinimide (3.54 g, 26.6 mmol) in DMF (25 mL) was stirred at 55 °C for 12 h under an N_2 atmosphere. After completion of the reaction as monitored by TLC, 20 mL of water and 10 mL of saturated sodium thiosulfate solution were added to the reaction mixture. After stirring at room temperature for 10 min, the precipitate formed was collected by filtration, washed with water, and dried under vacuum to afford a yellow powder. (1.1 g, 42.0% yield). ^{1}H-NMR (400 MHz, DMSO-d_6) δ: 14.32 (s, 1H), 8.37 (s, 1H); *m/z*: 148.1 $[M + H]^+$.

General procedure for the synthesis of compounds 1a–u, 1w–z, 4a–c (exemplified by 1a)

A mixture of 3-Nitro-1*H*-pyrazole (1.0 g, 8.9 mmol), 2, 4-dichlorobenzyl chloride (1.9 g, 9.7 mmol), potassium carbonate (3.7 g, 26.7 mmol), and tetrabutylammonium bromide (145 mg, 0.89 mmol) in *N*, *N*-dimethylformamide was stirred at room temperature for 1 h. After completion of the reaction as monitored by TLC, 10 mL of water was added to the reaction mixture. The resulting precipitate was collected by filtration, washed successfully with water, saturated brine, and then dried under vacuum to afford a white solid. Yield: 94%, white solid; ^{1}H-NMR (400 MHz, DMSO-d_6) δ: 8.16 (d, J = 2.4 Hz, 1H), 7.71 (d, J = 2.0 Hz, 1H), 7.49 (dd, J = 8.4, 2.0 Hz, 1H), 7.30 (d, J = 8.4 Hz, 1H), 7.11 (d, J = 2.4 Hz, 1H), 5.59 (s, 2H); MS (ESI), *m/z*: 272.1 $[M + H]^+$.

Additional data for characterization of all target compounds **1b–z**, **4a–c** can be found in Appendix S1.

Biological experiments

Cell culture and necroptosis induction

HT29 was cultured in Dulbecco's modified Eagle's medium supplemented with 10% fetal calf serum (FCS), L-glutamine (200 mM), and sodium pyruvate (400 mM). Necroptosis was induced by 20 ng/mL TNF-α (PEPROTECH, Rocky Hill, NJ, USA), 100 nM Smac mimetic (SELLECK), and 20 μM Z-VAD-FMK (APExBIO, Houston, TX, USA).

Kinase binding assay

The kinase binding affinity of compounds was measured through the KINOMEscan™ kinase binding assay (DiscoveRX). In this assay, the binding affinity of a compound to a kinase is calculated by quantitatively measuring the competition binding ability of this compound and an immobilized, active-site-directed ligand with the kinase.

Immunoprecipitation and Western Blot

HT29 cells at 90% confluence grown were washed once with PBS and lysed for 20 min on ice in the RIPA lysis buffer (Beyotime, Jiangsu, China). Cell lysates were centrifuged at 16060× *g*. The solution fraction was collected, and protein concentration was determined by BCA Protein Assay kit (Beyotime). Then, 1 mg of the extracted protein was immunoprecipitated overnight with antiphosphoserine (Invitrogen, Camarillo, CA, USA) at 4 °C and then captured by protein A agarose (Roche, Mannheim, Germany) for another 6 h. Next, the agarose was washed three times with PBS and then boiled in 1% SDS loading buffer, and the supernatant was conducted Western blot with RIP1 (BD) and RIP3 (ABcam, Cambridge, UK). The other antibodies, p-MLKL and MLKL, were purchased from ABcam and β-actin was from ZSGB-BIO.

Animal experiments

Specific pathogen-free male C57BL/6 mice (weight 20–24 g) were supplied from experimental animal center of Sichuan University. Mice after overnight fasting were injected with 8% L-arginine (dissolved in saline, PH = 7.3, 50 μL/g) by i.p. twice in an hour. For drug administration, compound **4b** was dissolved in drinking water with 12.5% alcohol and 12.5% castor oil. The mice were killed after

5 days drug administration. To evaluate the changes in pancreas histology, sections of paraformaldehyde-fixed pancreas tissues were stained with hematoxylin and eosin (HE) and photographed by an optical microscope.

Results and Discussion

Chemistry

A total of 28 1-benzyl-1*H*-pyrazole derivatives were synthesized and synthetic routes of these compounds are outlined in Schemes 1 and 2. As shown in Scheme 1, compounds **1a**–**u** and **1w**–**z** were obtained through reactions of commercial available reagents containing chloromethyl or bromomethyl with pyrazoles in the presence of alkali in excellent yields. **1s** was stirred with *N*-methylpiperazine in an alkaline condition to give compound **1v**. Scheme 2 depicts the synthetic routes for compounds **4a**–**c**. 3-nitropyrazole underwent halogenation reactions with halogenated reagents to produce intermediates **3a**–**c**, which then reacted with 2, 5-difluorobenzyl bromide in the presence of alkali to afford final products **4a**–**c**.

Necroptosis inhibitory activities and structure-activity relationships

The SAR analysis below will be based on the cell necroptosis inhibitory assay rather than a direct enzymatic assay, which is due to the following reasons. A SAR analysis based on cellular assays may permit the evaluation of both the intrinsic activity of compounds against the protein target and the ability of compounds to permeate the cell wall. In addition, relative to the enzymatic assay, the cell-based assay is much cheaper. For the most potent compound in the cell-based assay, its enzymatic activity will be measured.

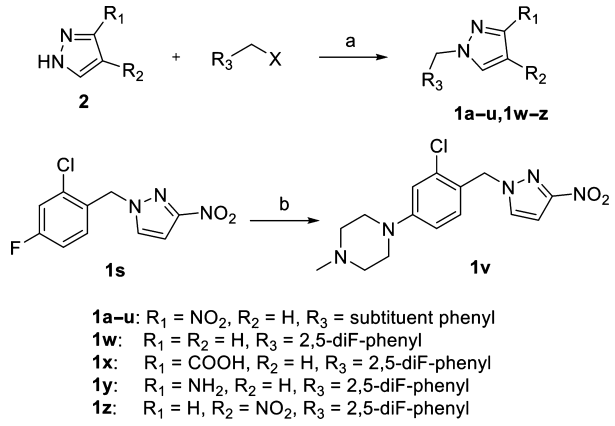

Scheme 1: Reagents and conditions: (a) reagents containing chloromethyl or bromomethyl, K_2CO_3, $Bu_4N^+Br^-$, DMF, rt, 2 h; (b) N-methylpiperazine, ethyldiisopropylamine, rt, overnight.

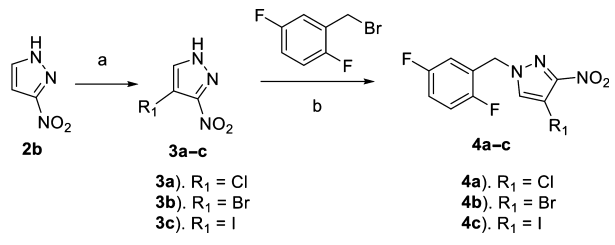

Scheme 2: Reagents and conditions: (a) NCS (or NBS/NIS), ethyldiisopropylamine, rt, overnight; (b) K_2CO_3, $Bu_4N^+Br^-$, DMF, rt, 1 h.

Substitution effect of benzyl

Table 1 shows the chemical structures of compounds **1a**–**v** and their bioactivities. Replacement of the benzene ring with benzoheterocycle or biphenyl abolished the bioactivity (EC_{50} > 10 μM, **1b**–**d**). A pure benzyl (without any substituent) resulted in a diminished activity (**1e**). Compound **1f**–**h** bearing a monosubstituted ortho-, meta- or para-chloride displayed one to three times lower activity than **1a**. When the para-chloride atom was replaced by more polar methoxyl, amino, or trifluoromethyl group, the bioactivity was further decreased (**1i**, **1j**, and **1k)**. Compounds **1l** and **1m**, which contain a monosubstituted para-bromide and ortho-methyl, respectively, also showed decreased bioactivity. However, compound **1n**, containing a bromide substituted at ortho position, exhibited about twofold higher potency than compound **1a**. Among compounds **1o**–**v**, which contain disubstituted benzyl, three compounds (**1p**, **1q** and **1s)** showed an increased bioactivity compared with **1a**. It is obvious that different substitution number and sites of halide (F, Cl, Br) on the benzene ring have some influence on the bioactivity of compounds. Compound **1q**, which bears two fluoride substituents at C-2 and C-5 positions of the benzene ring, corresponds to the most active compound (EC_{50}: 0.290 μM).

Influence of substituents of pyrazole

In this section, we shall discuss the influence of substituents of pyrazole with the benzyl moiety fixed as its optimal substituents, namely 2,5-difluorobenzyl. For this purpose, a total of seven compounds were synthesized (see Table 2). Compound **1w** with no any substituent on the pyrazole ring showed a significantly decreased bioactivity compared with compound **1q**. Replacement of nitro by carboxylate or amino also led to reduced bioactivity (**1x**, **1y**). Translocation of nitro from the C-3 position to the C-4 position (**1z**) resulted in a significantly decreased bioactivity. Introduction of a chlorine or bromine atom at the C-4 position of pyrazole ring slightly increased the bioactivity (**4a** and **4b**), and introduction of an iodine atom led to a weakly decreased bioactivity (**4c**).

The above SAR studies led to the discovery of compound **4b**, which displayed the most potent activity in the cell necroptosis inhibitory assay. Then, the enzymatic activity of **4b** was measured by the KINOMEscan™ kinase binding assay. In this assay, compound **4b** showed a K_d value of 0.078 μM. For comparison, the enzymatic activity of Nec1

was also measured at the same experimental condition, which gave a K_d value of 0.130 μM, indicating that compound **4b** is a little more potent than Nec1.

Table 1: Structures of compounds **1a**–**v** and their bioactivities

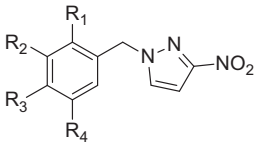

Compound	R1	R2	R3	R4	EC_{50}[a](μM)
1a	Cl	H	Cl	H	1.048 ± 0.117
1b	-CH=CH-CH=CH-		H	H	>10
1c	-O-CH2-CH2-O-		H	H	>10
1d	H	H	4-cyanophenyl	H	>10
1e	H	H	H	H	2.463 ± 0.072
1f	Cl	H	H	H	2.543 ± 0.026
1g	H	Cl	H	H	3.240 ± 0.277
1h	H	H	Cl	H	1.449 ± 0.129
1i	H	H	OCH3	H	5.940 ± 0.181
1j	H	H	NH2	H	5.603 ± 0.432
1k	H	H	CF3	H	7.371 ± 0.522
1l	H	H	Br	H	1.955 ± 0.092
1m	CH3	H	H	H	1.158 ± 0.052
1n	Br	H	H	H	0.550 ± 0.073
1o	H	F	F	H	3.012 ± 0.288
1p	F	H	F	H	0.881 ± 0.007
1q	F	H	H	F	0.290 ± 0.003
1r	H	F	H	F	1.872 ± 0.134
1s	Cl	H	F	H	0.827 ± 0.014
1t	Cl	H	H	Cl	5.880 ± 0.354
1u	F	H	H	Cl	3.671 ± 0.218
1v	Cl	H	Methylpiperazine	H	>10

[a]All assays were conducted in duplicate.

Table 2: Structures of compounds **1q**, **1w**–**z**, **4a**–**c** and their bioactivities

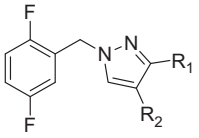

Compound	R1	R2	EC_{50}[a](μM)
1q	NO2	H	0.290 ± 0.003
1w	H	H	>10
1x	COOH	H	0.421 ± 0.019
1y	NH2	H	>10
1z	H	NO2	>10
4a	NO2	Cl	0.179 ± 0.006
4b	NO2	Br	0.160 ± 0.002
4c	NO2	I	0.413 ± 0.015
Nec1			0.860

[a]All assays were conducted in duplicate.

Protein-ligand docking studies

To understand the interaction mode of **4b** with RIP1, molecular docking was performed based on the crystal structure of RIP1 (PDB code: 4ITJ). Here, GOLD v5.0 was used for the docking studies (19,20). The predicted binding mode is shown in Figure 3. **4b** suitably resides in the allosteric pocket of RIP1 kinase. Two hydrogen bonds are formed between the 4-bromo-3-nitro-1*H*-pyrazole moiety of **4b** and residue Asp156 of the RIP1 kinase. The 2,5-difluorobenzyl moiety of **4b** locates in a hydrophobic pocket formed by a number of hydrophobic residues including Leu157, Ala155, Val76, Ile154, and Met92.

Inhibitory effect on necroptotic signaling

Western blot assays were performed to examine the signaling inhibition ability of **4b** in intact cells. In these assays, HT29 cells were treated with TSZ by 8 h. The results showed that the phosphorylation of MLKL (p-MLKL) was inhibited by **4b** in a concentration-dependent manner (Figure 4A). Because there is no commercially available phosphorylated RIP1 (p-RIP1) and RIP3 (p-RIP3) antibodies, immunoprecipitation was performed to detect the levels of phosphorylated RIP1 and RIP3, in which antiphosphoserine antibody and protein A agarose were used to pull down p-RIP1 and p-RIP3(21). The results (see Figure 4B) indicated that **4b** inhibited the phosphorylation of RIP1 and RIP3 in a concentration-dependent manner. Overall, our results demonstrated that **4b** could dose dependently inhibit the activation of RIP1/RIP3/MLKL signaling in intact cells.

The protective effect on pancreas in an L-arginine-induced pancreatitis mouse model

Finally, an L-arginine-induced pancreatitis mouse model was used to examine the *in vivo* effect of **4b**. Excessive doses of L-arginine could reduce polyamine biosynthesis

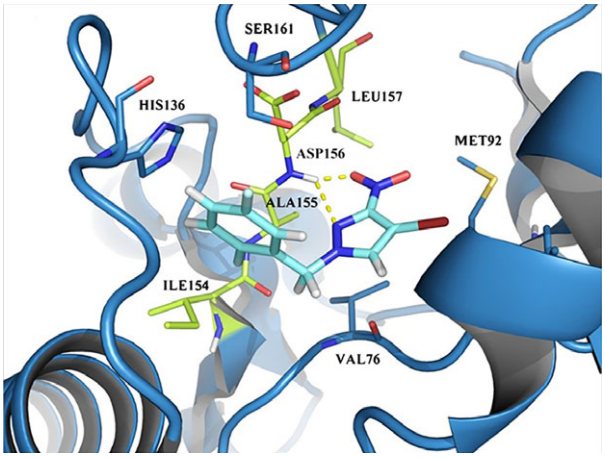

Figure 3: The predicted binding mode of **4b** with the RIP1 kinase.

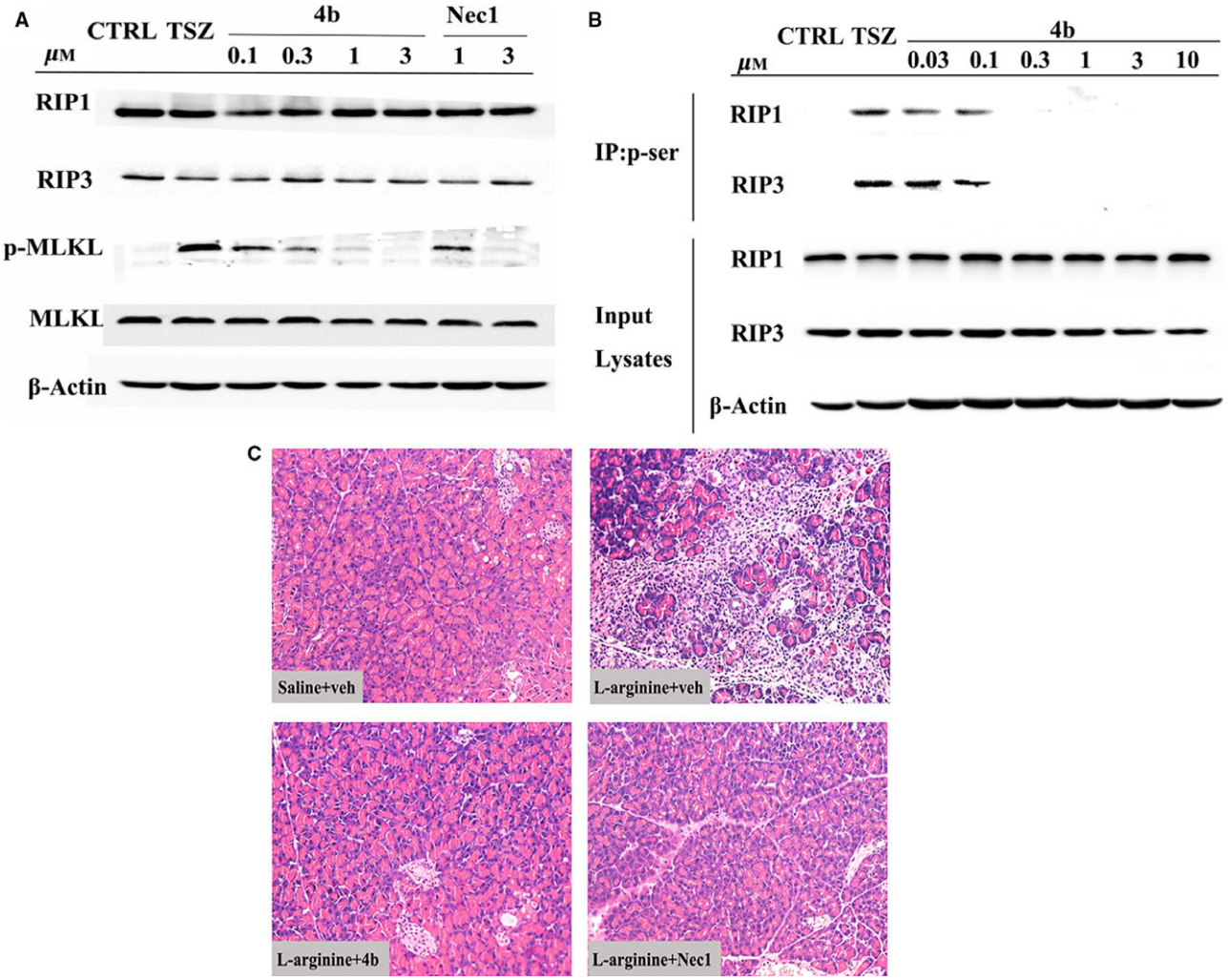

Figure 4: (A) Western Blot conducted in HT29 after TSZ inducing to measure RIP1, RIP3, MLKL, and p-MLKL with **4b** or Nec1 treated. (B) Immunoprecipitation performed with antiphosphoserine and protein A agarose to capture p-RIP1 and p-RIP3, blotted with RIP1 and RIP3 antibody in HT29 cells. (C) HE staining of paraffin section of pancreas with or without L-arginine injection and **4b** or Nec1 administration.

and thus inhibit the synthesis of protein. The pancreatic acinar cells have the most active protein synthesis and would be injured by administration of large doses of L-arginine. In this model, C57BL/6 mice after overnight fasting were injected with 8% L-arginine (dissolved in saline and the dosage is 50 μL/g) two times interval of an hour. Then **4b** or Nec1 was administrated by i.p. 10 mg/kg/day for 5 days. Mice were killed on the sixth day, and pancreas damage was evaluated by HE staining. As shown in Figure 4C, **4b** displayed a considerable pancreas-protecting effect in the L-arginine-induced pancreatitis mouse model (22).

Conclusion

In summary, SAR analysis led to the discovery of a potent RIP1 kinase inhibitor, **4b**, which contains a new scaffold of 1-Benzyl-1*H*-pyrazole. This compound showed an EC_{50} value of 0.160 μM in the cell necroptosis inhibitory assay and a K_d value of 0.078 μM against the RIP1 kinase. It also exhibited considerable ability to inhibit the RIP1/RIP3/MLKL signaling in intact cells and showed a good protective effect on pancreas in the L-arginine-induced pancreatitis mouse model. Overall, compound **4b** could be taken as a good lead compound for further studies.

Acknowledgments

This work was supported by the 973 Program (2013CB967204), and the National Natural Science Foundation of China (81172987, 81325021, 81473140), and partly by the National Science and Technology Major Project (2012ZX09501001-003, 2012ZX09102-101-002), and PCSIRT (IRT13031).

References

1. You Z., Whalen M. (2005) Traumatic brain injury in mice deficient in tumor necrosis factor receptor-2 and FAS: effects on histopathology and functional outcome. J Neurotraum;22:1227.
2. Yuan J., Lipinski M., Degterev A. (2003) Diversity in the mechanisms of neuronal cell death. Neuron;40:401–413.
3. Lim S.Y., Davidson S.M., Mocanu M.M., Yellon D.M., Smith C.C.T. (2007) The cardioprotective effect of necrostatin requires the cyclophilin-d component of the mitochondrial permeability transition pore. Cardiovasc Drug Ther;21:467–469.
4. Mareninova O.A., Sung K.F., Hong P., Lugea A., Pandol S.J., Gukovsky I., Gukovskaya A.S. (2006) Cell death in pancreatitis: caspases protect from necrotizing pancreatitis. J Biol Chem;281:3370–3381.
5. Upton J.W., Kaiser W.J., Mocarski E.S. (2008) Cytomegalovirus M45 cell death suppression requires receptor-interacting protein (RIP) homotypic interaction motif (RHIM)-dependent interaction with RIP1. J Biol Chem;283:16966–16970.
6. Degterev A., Huang Z.H., Boyce M., Li Y.Q., Jagtap P., Mizushima N., Cuny G.D., Mitchison T.J., Moskowitz M.A., Yuan J.Y. (2005) Chemical inhibitor of nonapoptotic cell death with therapeutic potential for ischemic brain injury. Nat Chem Biol;1:112–119.
7. Cho Y., Challa S., Moquin D., Genga R., Ray T.D., Guildford M., Chan F.K.M. (2009) Cell;137:1112.
8. Christofferson D.E., Li Y., Yuan J.Y. (2014) Control of life-or-death decisions by RIP1 kinase. Annu Rev Physiol;76:129–150.
9. Feoktistova M., Geserick P., Kellert B., Dimitrova D.P., Langlais C., Hupe M., Cain K., MacFarlane M., Hacker G., Leverkus M. (2011) cIAPs block ripoptosome formation, a RIP1/caspase-8 containing intracellular cell death complex differentially regulated by cFLIP isoforms. Mol Cell;43:449–463.
10. Degterev A., Hitomi J., Germscheid M., Ch'en I.L., Korkina O., Teng X., Abbott D., Cuny G.D., Yuan C., Wagner G., Hedrick S.M., Gerber S.A., Lugovskoy A., Yuan J. (2008) Identification of RIP1 kinase as a specific cellular target of necrostatins. Nat Chem Biol;4:313–321.
11. Christofferson D.E., Yuan J.Y. (2010) Necroptosis as an alternative form of programmed cell death. Curr Opin Cell Biol;22:263–268.
12. Teng X., Degterev A., Jagtap P., Xing X.C., Choi S., Denu R., Yuan J.Y., Cuny G.D. (2005) Structure-activity relationship study of novel necroptosis inhibitors. Bioorg Med Chem Lett;15:5039–5044.
13. Jagtap P.G., Degterev A., Choi S., Keys H., Yuan J.Y., Cuny G.D. (2007) Structure-activity relationship study of tricyclic necroptosis inhibitors. J Med Chem;50:1886–1895.
14. Teng X., Keys H., Jeevanandam A., Porco J.A., Degterev A., Yuan J.Y., Cuny G.D. (2007) Structure-activity relationship study of [1,2,3]thiadiazole necroptosis inhibitors. Bioorg Med Chem Lett;17:6836–6840.
15. Wang K., Li J.F., Degterev A., Hsu E., Yuan J.Y., Yuan C.Y. (2007) Structure-activity relationship analysis of a novel necroptosis inhibitor, Necrostatin-5. Bioorg Med Chem Lett;17:1455–1465.
16. Wu Z.J., Li Y., Cai Y., Yuan J.Y., Yuan C.Y. (2013) A novel necroptosis inhibitor-necrostatin-21 and its SAR study. Bioorg Med Chem Lett;23:4903–4906.
17. Harris P.A., Bandyopadhyay D., Berger S.B., Campobasso N., Capriotti C.A., Cox J.A., Dare L. *et al.* (2013) Discovery of small molecule RIP1 kinase inhibitors for the treatment of pathologies associated with necroptosis. Acs Med Chem Lett;4:1238–1243.
18. Sun L.M., Wang H.Y., Wang Z.G., He S.D., Chen S., Liao D.H., Wang L., Yan J.C., Liu W.L., Lei X.G., Wang X.D. (2012) Mixed lineage kinase domain-like protein mediates necrosis signaling downstream of RIP3 kinase. Cell;148:213–227.
19. Verdonk M.L., Cole J.C., Hartshorn M.J., Murray C.W., Taylor R.D. (2003) Improved protein-ligand docking using GOLD. Proteins;52:609–623.
20. Verdonk M.L., Chessari G., Cole J.C., Hartshorn M.J., Murray C.W., Nissink J.W.M., Taylor R.D., Taylor- R. (2005) Modeling water molecules in protein-ligand docking using GOLD. J Med Chem;48:6504–6515.
21. Oerlemans M.I.F.J., Liu J., Arslan F., den Ouden K., van Middelaar B.J., Doevendans P.A., Sluijter J.P.G. (2012) Inhibition of RIP1-dependent necrosis prevents adverse cardiac remodeling after myocardial ischemia-reperfusion *in vivo*. Basic Res Cardiol;107:1–13.
22. Czako L., Takacs T., Varga I.S., Hai D.Q., Tiszlavicz L., Hegyi P., Mandi Y., Matkovics B., Lonovics J. (2000) The pathogenesis of L-arginine-induced acute necrotizing pancreatitis: inflammatory mediators and endogenous cholecystokinin. J Physiol Paris;94:43–50.

Supporting Information

Additional Supporting Information may be found in the online version of this article:

Appendix S1. Chemical characterizations of compounds 1b-1z, 3b-3c, 4a-4c.